Infection and Drug Resistance

Dovepress
Taylor & Francis Group

Open Access Full Text Article

ORIGINAL RESEARCH

Sporothrix schenckii Peptidorhamnomannan-Associated Protein 2 (Pap2) Is Involved in Adhesion and Virulence

Dario A Baruch-Martínez[1], Manuela Gómez-Gaviria[1], Joaquín O Chávez-Santiago[1], Uriel Ramírez-Sotelo[1], Luisa M Contreras-López[1], Iván Martínez-Duncker[2], Andréa Regina Souza Baptista[3], Héctor M Mora-Montes[1]

[1]Departamento de Biología, División de Ciencias Naturales y Exactas, Campus Guanajuato, Universidad de Guanajuato, Guanajuato, Gto, Mexico; [2]Laboratorio de Glicobiología Humana y Diagnóstico Molecular, Centro de Investigación en Dinámica Celular, Instituto de Investigación en Ciencias Básicas y Aplicadas, Universidad Autónoma del Estado de Morelos, Cuernavaca, Mor, Mexico; [3]Centro de Investigação de Microrganismos, Instituto Biomédico, Universidade Federal Fluminense, Niterói, RJ, Brazil

Correspondence: Héctor M Mora-Montes, Email hmora@ugto.mx

Introduction: The *Sporothrix schenckii* cell wall has been widely studied to understand its role in pathogenesis and the infection process. Previously, a component of the cell wall, the peptidorhamnomannan (PRM), was analyzed, and some proteins with unknown function were identified. Among them, the protein encoded by the SPSK_06559 gene stood out for its high abundance within PRM.
Methods: In this work, in silico analyses were performed to predict the adhesive properties of the SPSK_06559 protein (renamed as Pap2) to extracellular matrix (ECM) components, such as fibrinogen, fibronectin, and type-I and type-II collagen. Subsequently, a recombinant Pap2 (rPap2) version was generated to obtain experimental evidence of its adhesive properties to ECM components. Finally, the role of Pap2 in pathogenesis was assessed in *Galleria mellonella* larvae.
Results: Bioinformatic analyses consistently suggested that Pap2 possesses adhesive properties. Prediction was experimental validated: rPap2 showed strong adhesion to ECM components. Immunization with rPap2 conferred significant protection to *G. mellonella* larvae against a lethal dose of *S. schenckii*. Furthermore, preincubation of fungal cells with anti-rPap2 antibodies drastically reduced their ability to kill the larvae.
Discussion: These findings demonstrate that the SPSK_06559 protein (Pap2) participates in the initial adhesion to host tissues. Induction of a protective response through immune priming with rPap2 suggest that Pap2 is a promising immunogenic antigen. Reduction of lethality upon blocking Pap2 confirms its essential role in pathogenesis, positioning it as a potential target for the development of new therapies and vaccines against sporotrichosis.
Keywords: cell wall, glycoproteins, immune priming, peptidorhamnomannan, recombinant protein

Introduction

Sporothrix schenckii, Sporothrix brasiliensis, and *Sporothrix globosa* are currently the main etiological agents of sporotrichosis, an implantation mycosis that affects the skin and subcutaneous tissues.[1–3] The disease is worldwide distributed, but countries like Japan, China, India, South Africa, Madagascar, Brazil, Peru, and Mexico report most of the human and animal cases of sporotrichosis.[3–6] It is recognized as a sapronosis and a zoonosis, the latter having domestic cats as the source of human infection. Epidemic outbreaks of zoonotic sporotrichosis have been recently reported, particularly in Brazil, Argentina, Chile, Colombia, Mexico, Panama, Paraguay, and Peru.[7] Different from *S. brasiliensis*, which is currently restricted to Brazil and countries sharing a geographical border with this nation,[3] *S. schenckii* and *S. globosa* are cosmopolitan species and are found in the Americas, Europe, Africa, Asia, and Oceania.[2,4]

The first case of sporotrichosis was reported in 1896 and was linked with *S. schenckii*, the only *Sporothrix* species known at that time.[8] It was not until 2007 that other *Sporothrix* species of medical relevance were identified.[9]

Received: 23 October 2025
Accepted: 21 December 2025
Published: 26 December 2025

Consequently, most of the biological and fundamental aspects of the disease and the causative agent, including pathogenic aspects, have been studied in *S. schenckii*.[10]

Similar to other fungal pathogens of medical relevance, *S. schenckii* has a repertoire of virulence factors that allow it to colonize and damage host cells and tissues. Dimorphism, melanin production, adhesins, secreted hydrolytic enzymes, biofilm production, extracellular vesicles, and strategies to disguise host immunity are among the most studied virulence factors in *S. schenckii*.[11,12] Cell adhesion to extracellular matrix (ECM) components, cell surface, and inert plastic surfaces has been reported in *S. schenckii*, but little information on the proteins with adhesive properties is currently available. *S. schenckii* yeast-like cells' adhesion to epithelial cells has been previously reported, and cell wall glycoproteins with a molecular weight ranging from 190 kDa to 80 kDa have been linked with adhesive properties.[13] *S. schenckii* can also bind to endothelial cells, but with no effect on the host cellular integrity.[14] Biofilm formation, which involves cell adhesion, has been reported on plastic surfaces and feline claws.[15,16] This virulence factor is found in the three clinically relevant *Sporothrix* species.[16] In terms of binding to ECM components, *S. schenckii* yeast-like cells showed the ability to bind type-I and type-II collagen, laminin, fibronectin, fibrinogen, and elastin.[17–21] Even though proteomic and transcriptomic analyses have been performed in cells from different *Sporothrix* species, the search for proteins with adhesive properties has proven to be a challenging endeavor.[22] Currently, there is a handful of adhesins that have been identified in *S. schenckii*. The cell wall protein Gp70, a moonlighting protein with enzyme activity of 3-carboxy-cis,cis-muconate cyclase, and adhesive properties, was the first adhesin recognized in this organism. The protein was linked to adhesion to the dermis of mouse tails[23] and fibronectin.[24] Genetic approaches indicated that Gp70 is involved in adhesion to fibronectin and laminin in both *S. schenckii* and *S. brasiliensis* yeast-like cells.[25,26] Pap1 and Hsp60 are two other cell wall proteins that have shown adhesion to laminin, elastin, fibrinogen, and fibronectin.[20] Pap1 showed additional adhesion to type-I and type-II collagen.[20] Recently, the Cbp1 protein was identified as an adhesin for type-I and type-II collagen.[21]

Defects in the glycosylation of cell wall proteins have been linked to reduced adhesion to ECM components, suggesting that proper glycoprotein synthesis is essential for *S. schenckii's* adhesive properties.[27] Chitin and β-glucans are the main components of the *S. schenckii* inner layer of the cell wall, while glycoproteins are abundant in the outermost layer.[28,29] The heterogeneous complex named peptidorhamnomannan (PRM) is one of the most abundant cell wall glycoproteins. This is composed of mannose (57%), rhamnose (33.5%), galactose (1%), and proteins (14.2%).[30] The peptidic portion contains 325 proteins, some of them of unknown predicted functions.[20] Since Hsp60, Pap1, and Cbp1 were identified as adhesins belonging to the cell wall PRM,[20] we hypothesize that other proteins found in this cell wall complex may have adhesive properties.

Here, we analyzed the protein Spsk_06559, an abundant component of PRM with unknown function.[20] This protein was here renamed as Pap2 (Peptidorhamnomannan-associated protein 2). To assess its role in *S. schenckii* pathogenesis, we generated a recombinant version of Pap2, generated polyclonal antibodies, and used them in blocking experiments when *S. schenckii* yeast-like cells were interacting with the host.

Materials and Methods

Strains and Culture Conditions

Strains ATCC MYA-4821 and ATCC MYA-4823 of *S. schenckii* and *S. brasiliensis*, respectively, were used in this study.[31,32] YPD broth (2% [*w/v*] gelatin peptone, 3% [*w/v*] dextrose, and 1% [*w/v*] yeast extract), pH 4.5 at 28°C, was used for conidia and hyphae propagation, while dimorphism to yeast-like cells was induced in the same medium with a pH of 7.8. Cultures were incubated at 37°C for 4 days.[33] *Escherichia coli* BL21 Star™ (DE3) (Thermo Fisher Scientific, Waltham, MA, USA) was used for recombinant protein expression. Bacteria were incubated at 37°C in LB broth (1% [*w/v*] gelatin peptone, 0.5% [*w/v*] yeast extract, and 0.5% [*w/v*] NaCl). Culturing media was supplemented with 100 μg mL^{-1} ampicillin (Sigma-Aldrich, St Louis, MO, USA) during the molecular cloning for transformant selection.

Expression of Recombinant Spsk_06559

S. schenckii yeast-like cells were harvested by centrifuging and used for the isolation of total RNA, using TRIzol® reagent (Invitrogen, Carlsbad, CA, USA). The cDNA was synthesized and purified by adsorption chromatography, as described.[34] The open reading frame (ORF) from *SPSK_06559* (702 bp) was amplified by PCR using the primer pairs 5´CTCGAGATGTCTGGCATCCCAGAGCTTCTTTA´ and 5´AAGCTTCTACTCTTTTTTTCCGTTCTTCTTGG3´ (underlined sequences represent additional *Xho*I and *Hind*III to direct cloning in the expression vector). The pJET 1.2/blunt vector (Thermo Fisher Scientific) was used for isolation and molecular identification of the amplicon, and then this was subcloned into the *Xho*I and *Hind*III sites of the expression vector pCold I (Takara BioInc, Kusatsu, Shiga, Japan), generating pCold-*PAP2*. For heterologous expression, strain BL21 (DE3) was transformed with pCold-*PAP2*, and cells were incubated in LB broth supplemented with 100 μg mL^{-1} ampicillin (Sigma-Aldrich) for 20 h at 37°C and orbital shaking at 180 rpm. One mL of this culture was inoculated in 200 mL of fresh LB broth and incubated at 37°C and orbital shaking at 180 rpm, until reaching an $OD_{600\ nm}$ = 0.4. For recombinant gene expression, different isopropyl-β-D-1-thiogalactopyranoside (IPTG) concentrations were added and incubated for 20 h at 15°C. The tested IPTG concentrations ranged from 0.1 to 5 mM, and 1.0 mM was found to be the best concentration for gene induction. At the end of the induction of gene expression, cells were collected by centrifuging for 20 min at 1,500 × *g* at 4°C and kept at −20°C until use.

Recombinant Pap2 Purification

Bacteria were pelleted by centrifuging and resuspended in 5 mL of buffer A (8 M urea, 10 mM Tris-HCl, 100 mM NaH_2PO_4, pH 8.0). Bacteria were mixed with ≤ 106 μm size glass beads (Sigma-Aldrich), shaken for 1 min in a vortex, and rested 1 min on ice. This procedure was repeated 5 times, followed by 3 cycles of freezing at −70°C and thawing at 35°C. This procedure generated a cell homogenate, which was centrifuged at 9,484 × *g* at 4°C for 10 min, and the supernatant was saved for protein purification. The supernatant was loaded onto a 10 mL Poly-Prep column (Bio-Rad, Hercules, CA, USA) with 2 mL of TALON Metal Affinity Resin (Jena Bioscience, Jena, Germany) as reported.[35] The column was washed with 6 mL of each buffer A at pH 8.0, 7.5, and 7.0, and then protein elution was achieved by passing 10 mL of each buffer A at pH 6.5, 5.4, and 4.5.[35] In all cases, 2 mL fractions were collected. The protein purity was inspected by SDS-PAGE in 12% (*w/v*) gels and stained with 1 mM dithiothreitol and 0.25 M KCl.[20,36] The recombinant protein was sliced out from gels, the polyacrylamide fragments were suspended in PBS at 4°C, and were shaken at 120 rpm to recover protein for passive diffusion. The protein purity was assessed with silver nitrate staining, as described.[37] The DC Protein Assay kit (Bio-Rad, Hercules, CA, USA) was used for protein quantification.

Generation of Polyclonal Anti-Pap2 Antibodies

We used a male New Zealand rabbit for polyclonal antibody generation as described.[35] A venous blood sample was withdrawn before the immunization scheme, centrifuged, and the preimmune serum was stored at −20°C and used as a negative control in all the immunological tests conducted in this study. The intramuscular immunization scheme consisted of the injection of 150 μg of purified recombinant Pap2 (rPap2) suspended in complete Freund's adjuvant (Thermo Fisher Scientific). After 2 weeks, 150 μg of rPap2 suspended in incomplete Freund's adjuvant (Thermo Fisher Scientific) were injected, and three additional booster shots were administered with a two-week periodicity. After two weeks, the animal was bled, the serum was collected, and globulins were precipitated with 76% (*w/v*) ammonium sulfate and dialyzed against NaCl 0.15 M.[35] Polyclonal antibodies were titrated by indirect ELISA, as described,[35] using rPap2 as an immobilized antigen in microplates. The preimmune and immune sera were used in serial dilutions from 1:100 to 1:102,400. The anti-rPap2 antibody titer was 1:6400.

Western Blotting Assays

Four-day-grown yeast-like cells were pelleted by centrifuging, washed twice with 25 mM Tris, 2 mM DTT, and 5 mM EDTA, suspended in 425–600 μm size glass beads (Sigma-Aldrich), and disrupted by applying 10 cycles of shaking 1 min in a vortex and resting for 30 sec on ice. Cell homogenates were centrifuged for 5 min at 9,485 × *g*, and the

proteins were recovered from the supernatant and kept at −20 °C. Aliquots containing 50 µg total protein were separated by SDS-PAGE in 12% (*w/v*) polyacrylamide gels at 120 V for 90 min, the separated proteins were electrotransferred onto a nitrocellulose membrane (Invitrogen) at 120 V for 1 h using the Mini Trans-Blot Cell system (Bio-Rad) and transfer buffer (25 mM Tris, 192 mM glycine, and 20% [*v/v*] methanol), and this was verified by staining with 0.5% (*w/v*) Ponceau S-Red, 1% (*v/v*) acetic acid.[38] The membrane was blocked with 5% (*w/v*) casein in PBS-0.05% (*v/v*) Tween 20 overnight at 4°C, then washed 3 times with PBS-0.05% (*v/v*) Tween 20, and incubated with anti-rPap2 for 2 h at room temperature at a working dilution of 1:3,200. The membrane was washed again 3 times with PBS-0.05% (*v/v*) Tween 20 and incubated for 2 h with the goat anti-rabbit IgG-HRP antibody (Sigma-Aldrich) diluted at 1:5,000. After washing again 3 times with PBS-0.05% (*v/v*) Tween 20, the membrane was incubated with 1 mg mL^{-1} 3, 3′-diaminobenzidine (Sigma-Aldrich) and 1% (*v/v*) hydrogen peroxide (Sigma-Aldrich). Image capture was performed with a GeneGenius (Bio Imaging Systems, Jackson, MI, USA). Controls of the immunoblotting included the use of the preimmune serum as the primary antibody or the intentional absence of primary antibody during the assay.

Analysis of Pap2 Three-Dimensional Structure

The predicted three-dimensional model of *S. schenckii* Pap2 (SPSK_06559) was retrieved from the UniProt database (accessed on May 14, 2025) in "Protein Data Bank" (.PDB) format.[39] The retrieved structural files were subsequently analyzed using PyMOL software (version 3.0) (https://www.pymol.org/), which enabled the visualization of protein three-dimensional structures. Pap2 was analyzed using CB-Dock (version 2.0),[40] which enabled the identification of the most probable binding cavity for potential interactions with other proteins. Docking analyses were performed using the HDOCK server (version 1.1).[41] This approach enabled the prediction of binding affinities between Pap2 and several ECM proteins, including thrombospondin-1 (UniProtKB: 1LSL), laminin (UniProtKB: 4YEQ), elastin (UniProtKB: P15502), fibrinogen (UniProtKB: 3GHG), fibronectin III (UniProtKB: 1FNF), type-I collagen (UniProtKB: 8K4W), and type-II collagen (UniProtKB: 9J1R). In addition, bovine serum albumin (BSA; UniProtKB: 4F5S), a plasma protein not associated with the ECM, was included as a negative control. All protein structures were obtained from the UniProt database and downloaded in . PDB format. Docking scores were used as a comparative metric between different docking complexes, where a more negative score indicated a more favorable binding model.[41] Additionally, confidence scores were considered: values above 0.7 suggested a high likelihood of molecular interaction; scores between 0.5 and 0.7 indicated a possible interaction; and scores below 0.5 suggested that binding was unlikely.[41] The resulting protein–protein complexes were visualized and analyzed using PyMOL to identify key interacting residues within the predicted binding sites.

Adhesion Assays

Polystyrene microtiter plates (Maxisorp, Nunc, Sigma-Aldrich) were coated with 1 µg per well of each of the following proteins: recombinant human fibronectin, recombinant human thrombospondin-1, human type-1 collagen, human laminin, human elastin, human fibrinogen, or bovine type-2 collagen (all from Sigma-Aldrich). The proteins were suspended in 0.2 M bicarbonate buffer, pH 9.4, dispensed in wells, and incubated overnight at 4°C. Then, plates were washed with PBS-0.05% (*v/v*) Tween 20 (PBS-Tween), and blocked with 1% (*w/v*) BSA, pH 7.4, for 2 h at 37°C. Plates were washed with PBS-Tween, 1×10^6 yeast-like cells were added per well, incubated for 1 h at 37°C, washed with PBS-Tween, and 100 µL of a rabbit anti-*S. schenckii* Hsp60 (1:3,000)[20] was added to each well, and plates were further incubated for 1 h at 37°C. Then, plates were washed with PBS-Tween, incubated with a goat anti-rabbit IgG-HRP antibody (Catalog number A0545; Sigma-Aldrich) 1:4000 in PBS-0.05% (*v/v*) Tween 20 for 2 h at room temperature, washed with PBS-Tween, and the reaction was developed with 0.5 mg/mL *o*-phenylenediamine and 0.005% [*v/v*] H_2O_2.[17] Color development was stopped after 5 min with 0.2 M H_2SO_4, and the absorbance at 490 nm was measured with a Varioskan LUX Multimode Microplate Reader (Thermo Fisher Scientific). In some experiments, yeast-like cells were preincubated with either anti-rPap2 or preimmune serum at a working dilution of 1:3,000 in PBS-0.05% (*v/v*) Tween 20 for 1 h at 37°C. Then, yeast-like cells were washed with PBS-Tween and included in adhesion assays described above.

E. coli cells expressing rPap2 were resuspended in 5 mL PBS, added with 50 mg mL^{-1} lysozyme (Sigma-Aldrich), incubated for 1 h at 37°C, 1% (*w/v*) SDS was added, and cells were incubated for 30 min at 37°C and shaken for 20 min in a vortex. The cell homogenate was centrifuged at 21,000 × *g* at 4°C, and 5 µg protein from the supernatant was used in

adhesion assays as described above, using anti-rPap2 antibody (1:3000) as primary antibody. Assays with the preimmune serum (1:3000) as primary antibody were included as a negative control. In both assays, wells coated only with BSA were used as controls.

Alternatively, HeLa cells (ATCC) growing as monolayer in Eagle's Minimum Essential Medium (Sigma-Aldrich) at 37°C and 5% CO_2 (v/v) were incubated with 0.25% (w/v) trypsin and 0.53 mM EDTA (Sigma-Aldrich),[20] cells were washed twice with PBS, concentration adjusted at 5×10^6 cells mL^{-1}, 200 µL were placed in microtiter plates, and incubated for 24 h at 37°C and 5% (v/v) CO_2. Plates were blocked and used in adhesion assays as mentioned above.

Ethical Statement

The use of *Galleria mellonella* larvae in this study was approved by the Ethics Committee of the University of Guanajuato (CEPIUG-P105-2023); while the use of one male New Zealand rabbit was approved under the reference code CEPIUG-P69-2023. Animal euthanasia was conducted as recommended by the American Veterinary Medical Association and the National guideline for laboratory animals (NOM-062-ZOO-1999). For rabbit euthanasia, we followed the recommended method of cervical dislocation, whilst *G. mellonella* larvae were cooled at 4°C until movement ceased before decapitation (point S2.4.3.2 and S7.2.2.3, respectively, of the American Veterinary Medical Association guidelines for euthanasia of animals: 2020 edition).

Virulence Assays in *Galleria mellonella* Larvae

Larvae were from a colony previously established in our laboratory[42] and were fed and hydrated ad libitum with a standard diet. Only larvae with a length between 1.2 and 1.5 cm, active and vigorous movements, and no body melanization were included in the study.[42] Control and experimental groups contained 30 larvae each. Injections were performed in the last left pro-leg, as reported.[42] The control group was injected with 10 µL PBS, while the experimental group was injected with 10 µL of 1×10^7 yeast-like cells mL^{-1}.[42] Larvae were housed at 37°C and were under daily observation for two weeks. Larvae with rigid and extensive body melanization, along with a lack of response to external stimuli, were considered dead. To quantify fungal colony-forming units (CFUs), dead larvae or those alive at the end of the experiment were decapitated, hemolymph collected, serially diluted, and incubated on YPD plates, as described.[43]

For quantification of immunological and cytotoxic parameters, groups of 10 larvae were inoculated as described above and incubated at 37°C for 24 h. Then, larvae were decapitated, hemolymph collected, anticoagulated, and used for hemocyte counting, cytotoxicity, melanin levels, and phenol oxidase activity.[44] Melanin was measured by spectrophotometry at 405 nm,[43] whilst cytotoxicity and phenoloxidase activity were measured in cell-free hemolymph, using the Pierce LDH Cytotoxicity Assay (Thermo Fisher Scientific), and 20 mM 3,4-dihydroxyDL-phenylalanine (Sigma-Aldrich), respectively.[43]

Bioinformatics Analyses

Disorder and signal peptide prediction were analyzed using the following sites: IUPred2A (https://iupred2a.elte.hu/; accessed on May 14, 2025)[45] and Protter (https://wlab.ethz.ch/protter/start/; accessed on May 14, 2025).[46] Hydrophobicity analysis Kyte-Doolittle and GRAVY were analyzed in the following sites: ProtScale (https://web.expasy.org/protscale/; accessed on May 14, 2025),[47] and ProtParam (https://web.expasy.org/protparam/; accessed on May 14, 2025),[47] respectively. Homologous search annotated as moonlighting proteins was performed using the MoonProt database (https://www.moonlightingproteins.org/search/; accessed on May 14, 2025).[48]

The conserved domain analyses and taxonomic distribution based on hidden Markov models were conducted on http://hmmer.org/ (accessed on May 14, 2025) using BLAST.[49] Sequence alignments in taxonomic distribution were performed with Clustal Omega (https://www.ebi.ac.uk/jdispatcher/msa/clustalo; accessed on May 14, 2025),[50] and their visualization using the https://alignmentviewer.org/ site; accessed on May 14, 2025. The conserved regions in structural comparisons were obtained utilizing the .pdb files retrieved from US-align with Chimera (Version 1.17.1) using the "Clustal Omega Alignment" plugin and choosing the option "select by conservation".

The phylogenetic reconstruction was generated with data retrieved from the NCBI database (https://ncbi.nlm.nih.gov/; accessed on May 14, 2025) and generated with MEGA (Version 11). Sequences retrieved from BLAST analysis were

aligned with ClustalW using default parameters. The analysis was performed using the maximum likelihood statistical method; bootstrap method and the number of bootstrap replications of 500 for the phylogeny test; JTT matrix-based model (Jones, Taylor, Thornton) for substitution of uniform rates for rates and patterns; use of all sites for data subset to use; for tree inference, the following options were applied: Nearest-Neighbor-Interchange (NNI) ML heuristic method, Neighbor-Joining initial tree for ML, and branch swap filter strong; and finally, number or threads of 1 for system resource usage.

Statistical Analysis

The GraphPad Prism 8 software was used to establish statistical significance. Data were assessed for normality using the Shapiro–Wilk test. Since the adhesion assays showed a normal distribution, these were analyzed with the *T*-test. Kaplan-Meier plots were used to show experiments in *G. mellonella* larvae, and these were analyzed with the Log rank test. Colony-forming units, hemocyte counting, melanin levels, cytotoxicity, and phenoloxidase activity were analyzed with the Mann–Whitney *U*-test, as their results did not show normality. In all cases, statistical significance was set at $P < 0.05$. All data are represented with mean and standard deviation.

Results

Production of Recombinant Pap2 and Immunodetection of Native and Recombinant Protein

To analyze the function of Pap2 during the pathogen-host interaction, we generated the recombinant version using *E. coli* BL21 cells and the plasmid pCold-*PAP2*. Several conditions for gene induction were tested (data not shown), and the best were using 1 mM isopropyl-β-D-1-thiogalactopyranoside and 20 h of incubation. Under these induction conditions, a 28.7 kDa protein band was observed in the cell homogenates of bacteria transformed with pCold-*PAP2*, corresponding to recombinant Pap2 (rPap2) (Figure 1A). The predicted Pap2 molecular weight is 25.3 kDa, and, likely, the discrepancy between experimental and predicted molecular weight may be due to the molecular tags added by the pCold I vector for protein purification. As a control, protein homogenates from untransformed *E. coli* BL21 cells and *E. coli* BL21 cells transformed with the empty pCold I vector were analyzed by SDS-PAGE (Figure 1A). None of the control homogenates showed overexpression of the protein (Figure 1A). Since 6X His is one of the molecular tags added by the plasmid to the recombinant protein, we purified the rPap2 by affinity chromatography. At the end of the purification protocol, only the rPap2 protein band was observed in the purified preparations (Figure 1B and C).

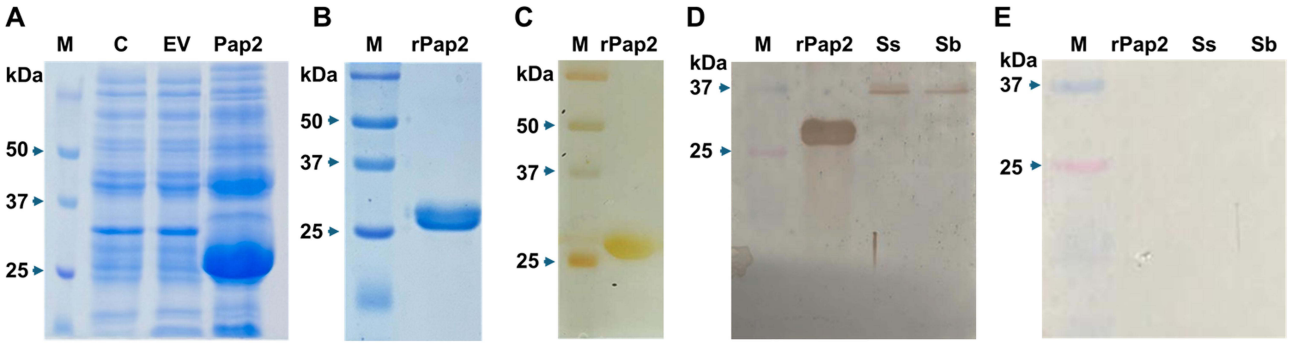

Figure 1 Expression of recombinant Pap2 expressed in *Escherichia coli* and immunodetection of native and recombinant Pap2. In (**A**) *E. coli* BL21 (DE3) cells were cultured under induction conditions. Cell homogenates were obtained, separated by denaturing SDS-PAGE on 12% (*w*/*v*) gels, and stained with Coomassie blue. M, molecular weight marker; C, untransformed *E. coli* BL21 (DE3) cells; EV, *E. coli* BL21 (DE3) transformed with the empty pCold I vector; Pap2, *E. coli* BL21 (DE3) transformed with pCold I-*PAP2*. In (**B**), the cell homogenates were subjected to protein purification using TALON Metal Affinity Resin. The fractions were evaluated by SDS-PAGE on 12% (*w*/*v*) gels and stained with Coomassie blue. M, molecular weight marker; rPap2, purified recombinant Pap2. In (**C**), the same sample as in panel (**B**) was used, but silver-stained. M, molecular weight marker; rPap2, purified recombinant Pap2. In (**D**) protein preparations were separated by SDS-PAGE on 12% (*w*/*v*) gels, transferred to a nitrocellulose membrane, and used in a Western blot assay using anti-rPap2 antibody as the primary antibody. M, molecular weight marker; rPap2, purified recombinant Pap2; Ss, *Sporothrix schenckii* yeast-like homogenate; Sb, *Sporothrix brasiliensis* yeast-like homogenate; In (**E**), same legend as in panel (**D**), but the Western blot was performed with preimmune serum as the primary antibody.

The purified recombinant protein was used to generate polyclonal antibodies in a rabbit. Once the antibodies were titrated, they were used to detect both native and recombinant Pap2 (Figure 1D). Immunoblotting assays with protein homogenates of *S. schenckii* and *S. brasiliensis* yeast-like cells showed a 37 kDa protein detected in both samples, suggesting that the native protein contains postranslational modifications that increase its molecular weight (Figure 1D). As a control, immunoblotting with the preimmune serum as primary antibody gave no detectable signal (Figure 1E).

Sporothrix schenckii Pap2 Has Adhesive Properties

The PRM is a heterogeneous complex of cell wall glycoproteins, and some of them have been characterized as adhesins.[20] So, it is feasible to conceive that Pap2 may also participate in adhesion to host components. We first used a bioinformatics approach to explore potential adhesive properties of Pap2. The putative three-dimensional structure of Pap2 is a barrel-like structure of beta-sheets with three small alpha helices surrounding the beta-sheets (Figure 2A). The analysis of this structure with the CB-Dock tool identified a putative superficial groove that might be involved in adhesion to other molecules (Figure 2A). Docking simulations using the HDOCK server showed that the Pap2 protein had theoretical values compatible with adhesion to laminin, fibrinogen, fibronectin, and type-I and type-II collagen (Table 1). It is known that *S. schenckii* does not bind to BSA or thrombospondin I.[17,19] Here, our bioinformatic approach showed low ability of Pap2 to interact with these proteins, stressing the usefulness of this approach (Figure 2B). A positive putative interaction between Pap2 and fibronectin is shown in Figure 2C. Therefore, the bioinformatic analysis indicates Pap2 may have adhesive properties.

Next, we performed an ELISA-based adhesion assay, using plates coated with different ECM components and *S. schenckii* yeast-like cells. The results were similar to previous adhesion profiles reported for *S. schenckii*,[17,19,20] ie, high binding to laminin and fibronectin, intermediate binding to elastin, type-I and type-II collagen, and low binding to fibrinogen (Figure 3A). The cells did not bind to thrombospondin-1, a result previously observed,[17,19,20] which validates our assay. We also included wells coated with HeLa cells to assess the ability of yeast-like cells to bind a whole epithelial cell, and the results showed a robust ability of fungal cells to bind this human cell line (Figure 3A). When assays were

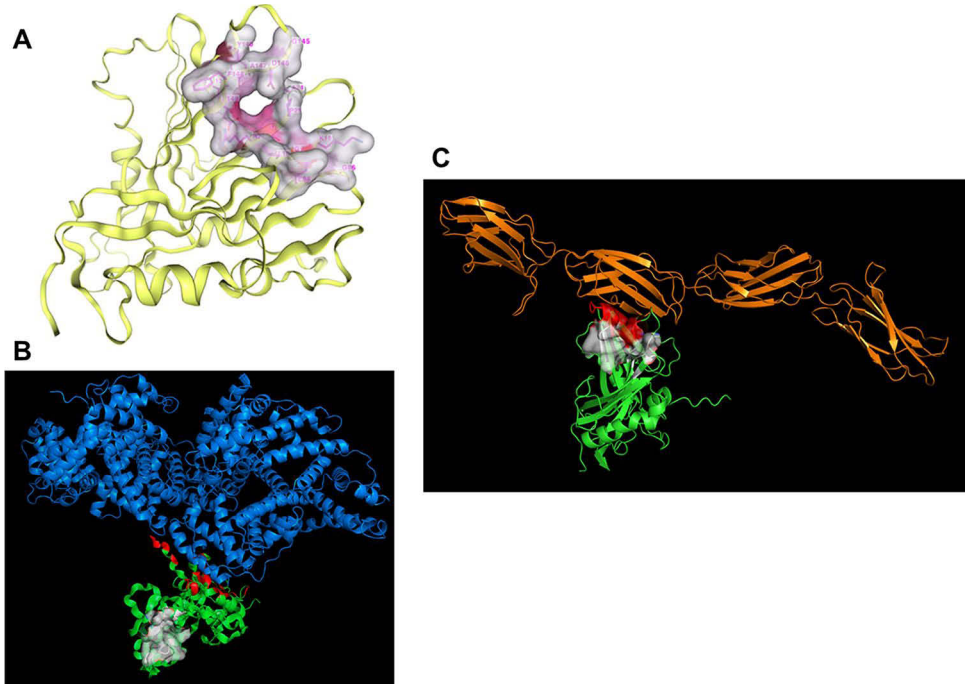

Figure 2 In silico analysis of adhesive properties of *Sporothrix schenckii* Pap2. In (**A**), Pap2 putative three-dimensional structure. The cloudy area indicates a putative superficial groove. Amino acids likely to be involved in adhesion to other molecules are highlighted in magenta. In (**B**) putative docking analysis of Pap2 (green) binding to bovine serum albumin (blue). In (**C**) putative docking analysis of Pap2 (green) binding to Fibronectin (Orange). In (**B**) and (**C**), red indicates the putative amino acids involved in binding, and a white cloud indicates the position of the superficial groove. The three panels were generated with PyMol.

https://doi.org/10.2147/IDR.S572598

Table 1 In silico Docking Analysis Between *Sporothrix schenckii* Pap2 and Selected Extracellular Matrix Proteins

Receptor	Ligand (PDB ID)	Docking Score[a]	Confidence Score[b]
Pap2	Thrombospondin I (1LSL)	−169,39	0,4804
	Bovine Serum Albumin (4F5S)	−186,63	0,4754
	Laminin (4YEQ)	−229,38	0,8303
	Elastin (P15502)	−228,52	0,8252
	Fibrinogen (3GHG)	−286,45	0,9219
	Fibronectin III (1FNF)	−292,19	0,8634
	Collagen type I (8K4W)	−233,9	0,7887
	Collagen type II (9J1R)	−217,7	0,7759

Notes: [a]A more negative docking score means a more possible binding model. [b]A confidence score above 0.7 indicates that the two molecules are likely to interact; a score between 0.5 and 0.7 indicates that the two molecules might interact; when the confidence score is below 0.5, the two molecules are unlikely to bind.

performed with yeast-like cells preincubated with anti-Pap2 antibody, there was a significant reduction in the ability to bind to laminin, elastin, fibrinogen, fibronectin, and HeLa cells (Figure 3A). Even though there was a trend of less binding to type-I and type-II collagen, the results were not significantly different from the untreated yeast-like cells (Figure 3A). Adhesion assays with fungal cells preincubated with preimmune serum showed a similar adhesion profile to untreated cells (Figure 3A), confirming that the changes in adhesion of the cells preincubated with anti-Pap2 antibody are because of the Pap2 blocking (Figure 3A). Control wells with only blocking agent (BSA) gave threshold readings (Figure 3A). Collectively, these data suggest that Pap2 may have adhesion properties.

To have additional evidence to support the role of Pap2 as an adhesin, we performed adhesion assays using cell homogenates from *E. coli* BL21 pCold-*PAP2*. Total protein extracts from non-transformed *E. coli* or those transformed with the empty pCold-I vector did not show binding to the ECM components tested (Figure 3B). Both showed a similar and modest ability to bind to HeLa cells (Figure 3B). Total protein extracted from cells expressing *PAP2* showed a modest ability to bind type-I and type-II collagen, laminin, and elastin (Figure 3B). However, this protein extract showed high adhesion to fibrinogen, fibronectin, and HeLa cells (Figure 3B). A control with heat-denatured protein extract containing rPap2 showed threshold readings similar to control wells where only BSA was included (Figure 3A). Collectively, these data support the role of Pap2 as an adhesin.

Pap2 Contributes to *Sporothrix schenckii* Virulence

Since Pap2 showed adhesive properties, we hypothesized that this protein may have a role in fungal virulence. We used an experimental sporotrichosis model in *G. mellonella* to assess virulence. Larvae inoculated with yeast-like cells showed a median survival of 6.0 ± 0.5 days and a mortality of 76.6 ± 6.5% (Figure 4). However, larvae inoculated with yeast-like cells preincubated with the anti-Pap2 antibody showed a median survival of more than 15 days and a mortality of 33.3 ± 5.8%. Larva inoculated with yeast-like cells preincubated with the preimmune serum showed a mortality of 79.8 ± 6.4% and median survival of 6.0 ± 1.0 days (Figure 4). When the fungal burden was analyzed in the hemolymph of inoculated larvae, we observed lower CFUs in the group infected with yeast-like cells preincubated with anti-rPap2 antibody, when compared to the groups inoculated with untreated cells or preincubated with preimmune serum (Table 2). In line with this observation, the animal group inoculated with cells preincubated with anti-rPap2 antibody showed lower cytotoxicity and levels of hemocytes, phenoloxidase activity, and melanin production (Table 2).

Pap2 Stimulates Immunological Priming in *Galleria mellonella*

It was previously reported that *S. schenckii* cell wall proteins, such as Gp70, Hsp60, and Pap1, stimulated immunological priming in *G. mellonella*, and this rendered the larvae resistant to a lethal infection with *S.schenckii* cells.[20,51] Thus, we hypothesize whether a similar situation may occur with Pap2. Groups containing 30 larvae were inoculated with different rPap2 concentrations, and survival was observed daily. After 5 days of inoculation, no mortality was recorded in any of

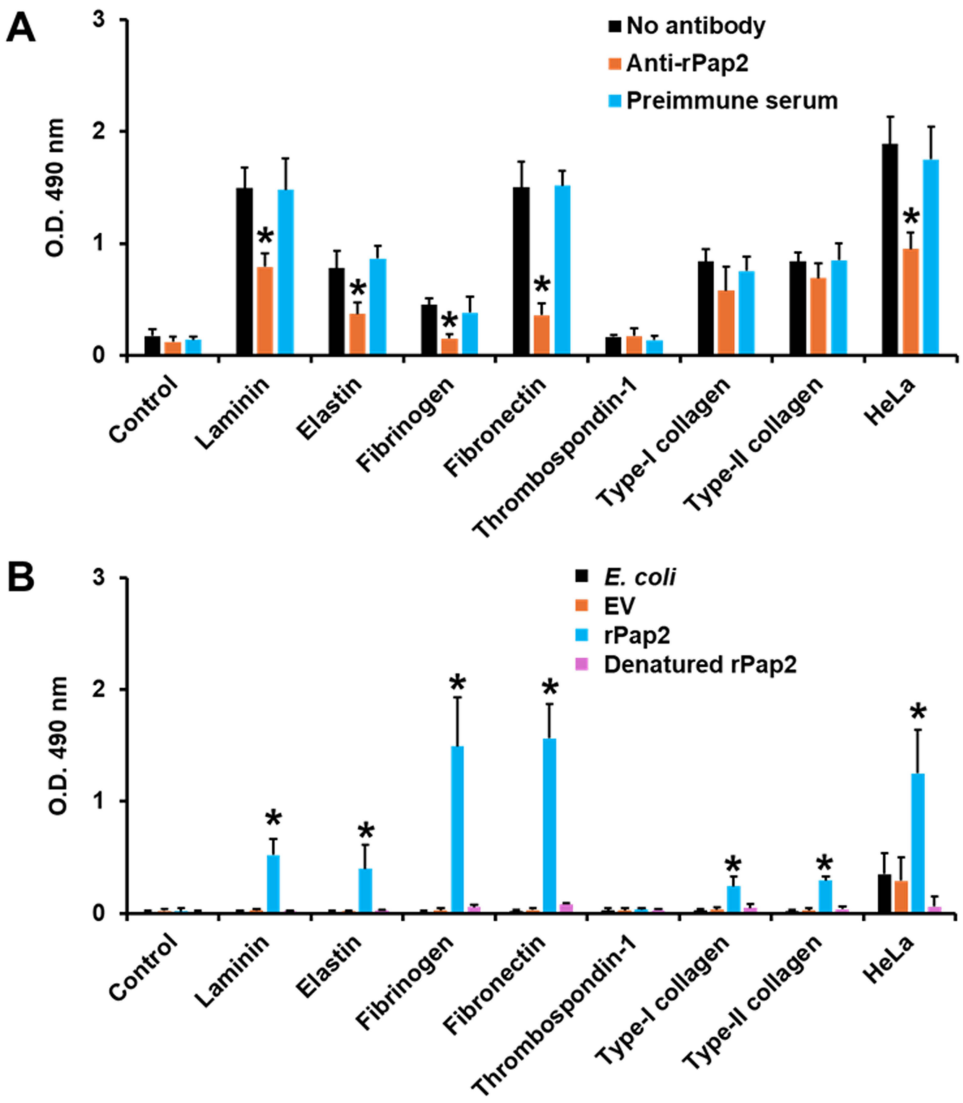

Figure 3 Adhesion to immobilized extracellular matrix components and HeLa cells. In (**A**) the extracellular matrix proteins or HeLa cells (HeLa) were immobilized onto 96-well plates and used in ELISA-based assays. Yeast-like cells were added to wells, and the binding to immobilized components was detected with anti-Hsp60 and the anti-rabbit IgG-HRP antibodies. No antibody, untreated *Sporothrix schenckii* yeast-like cells; Anti-rPap2, yeast-like cells preincubated with the anti-rPap2 antibody before interaction with immobilized compounds; Preimmune serum, yeast-like cells preincubated with the preimmune serum before interaction with immobilized compounds. The results are means ± SD of three independent experiments performed in duplicate. *$p < 0.05$ when compared to untreated yeast-like cells (No antibody). In (**B**) Total protein from *Escherichia coli* was added to 96-well plates coated with extracellular matrix proteins or HeLa cells (HeLa), and the protein-immobilized component interactions were detected with the anti-rPap2 antibody and the anti-rabbit IgG-HRP antibody. *E. coli*; protein from untransformed cells; EV, protein from cells transformed with the empty pCold-I vector; rPap2, protein from cells transformed with pCold-*PAP2* grown under induction conditions; Denatured rPap2, protein from cells expressing *PAP2* incubated at 100°C for 10 min before the adhesion assay. The results are means ± SD of three independent experiments performed in duplicate. *$p < 0.05$ when compared to *E. coli*, EV, and Denatured rPap2 groups.

the groups (data not shown). Then, hemolymph was collected, and hemocyte, melanin, and phenoloxidase levels were measured (Figure 5). The inoculation of 10 µg rPap2 did not show changes in these immunological parameters. However, the inoculation of 20–160 µg protein increased hemocyte levels, melanin production, and phenol oxidase activity in a dose-response way (Figure 5A and B). These data suggested immunological priming.[52,53] To assess whether this immunological priming may provide an advantage to larvae when interacting with *S. schenckii* yeast-like cells, groups of 30 larvae were inoculated with different concentrations of rPap2, incubated for 5 days, and then challenged with a lethal inoculum of *S. schenckii* cells. Similar to the results shown in Figure 4, the larva group inoculated with PBS and then challenged with fungal cells showed a mortality of 76.6 ± 4–5% and median survival of 6.0 ± 1.0 days (Figure 6). The inoculation of 10 µg rPap2 did not show any effect on the mortality curve; however, the injection of 20 µg rPap2 changed the mortality curve, with mortality of 66.6 ± 3.7% and a median survival of 9.0 ± 0.5 days (Figure 6). The inoculation of

https://doi.org/10.2147/IDR.S572598

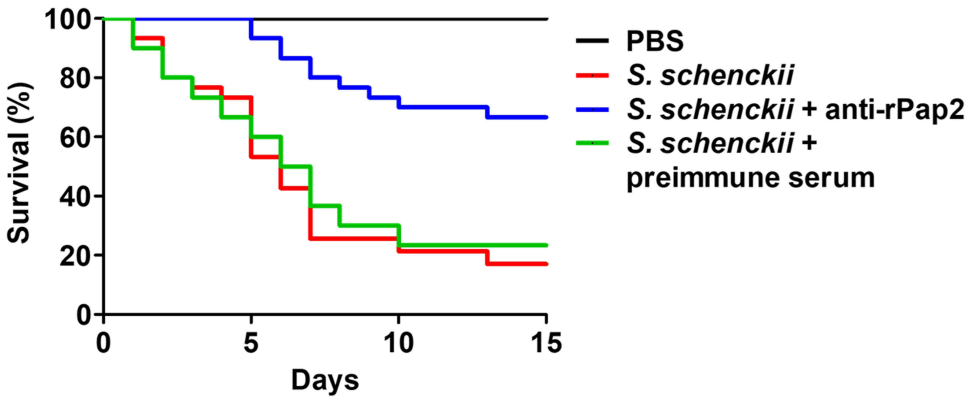

Figure 4 Virulence of *Sporothrix schenckii* yeast-like cells in *Galleria mellonella* larvae. Groups of 30 larvae were injected with yeast-like cells or phosphate buffer saline (PBS). Fungal cells were untreated or preincubated with anti-rPap2 antibody or preimmune serum before being used in the virulence assays. Larvae were observed for two weeks, and mortality was recorded daily.

40 µg rPap2 showed greater protection of larvae, as the mortality of the group was 30.0 ± 4.8% and a median survival of more than 15 days (Figure 6). The inoculation of 80 or 160 µg rPap2 showed a similar effect on larvae; the groups showed a mortality of 6.6 ± 3.8% with a median survival of more than 15 days (Figure 6). This dose-response effect observed in the mortality and median survival was replicated in the CFUs collected from challenged larvae, and the cytotoxicity, with a significant reduction in both parameters when larvae were inoculated with 20–180 µg rPap2 (Table 3). In the case of hemocytes, melanin, and phenoloxidase activity, these showed a positive dose-response trend, significantly increasing when groups were inoculated with 20–180 µg rPap2 (Table 3). Collectively, these data indicated that rPap2 stimulates a protective immunological priming that protects *G. mellonella* against *S. schenckii*.

Bioinformatics Analyses of *Sporothrix schenckii* Pap2

Since Pap2 is predicted to have an unknown function, we performed bioinformatics analyses aiming to predict its putative function, besides the adhesive properties described above. The analyses indicated that it does not contain a putative transmembrane domain or signal peptide; it has two disordered regions (amino acids 112 to 125 and 225 to 233), and a Gravy score of −0.489, indicating it is a hydrophilic protein. All these features are typical of cytosolic proteins. The analysis in the MoonProt database gave no relevant hints, suggesting this is not a moonlighting protein already reported in other organisms.

We also searched for functional domains in the Pap2 amino acid sequence using the ScanProsite tool (https://prosite.expasy.org/scanprosite/) and InterPro (https://www.ebi.ac.uk/interpro/) with no positive results. In the HMMER site (http://hmmer.org/), there were results indicating that Pap2 may have partial similarity to a NAD(p)-binding oxidoreductase from *Staphylotrichum logicolle*. No other domains could be predicted. Finally, the phylogenetic analysis indicated that it is a protein widely distributed in Ascomycota, with 517 genera possessing a putative homolog of *S. schenckii* Pap2 (data not shown).

Table 2 Colony-Forming Units, Cytotoxicity, Hemocyte Counting, Melanin, and Phenoloxidase Levels in *Galleria mellonella* Larvae Infected with *Sporothrix schenckii* Yeast-Like Cells

Inoculum	Colony-Forming Units ($\times 10^5$) [a]	Cytotoxicity (%)[b]	Hemocytes ($\times 10^6$) mL^{-1}	Melanin[c]	Phenoloxidase[d]
PBS	0.0 ± 0.0	10.7 ± 6.5	3.9 ± 0.4	1.6 ± 0.4	0.3 ± 0.3
Untreated cells	4.4 ± 0.5	92.8 ± 5.8	9.1 ± 0.6	5.8 ± 0.3	4.3 ± 0.6
+ anti-rPap2 antibody	2.2 ± 0.3	33.8 ± 12.5*	4.1 ± 0.8*	2.4 ± 0.6*	2.2 ± 0.4*
+ preimmune serum	4.6 ± 0.8	88.7 ± 6.9	8.7 ± 0.6	5.4 ± 0.7	4.6 ± 0.8

Notes: [a] Hemolymph was withdrawn from decapitated larvae and used to quantify fungal colony-forming units by serial dilutions in YPD medium. [b]Lactate dehydrogenase activity was quantified in cell-free hemolymph. The 100% activity corresponds to data obtained with lysed hemocytes. [c] Quantified in the cell-free hemolymph as A_{405nm}. [d] Phenoloxidase activity defined as the Δ_{490nm} min^{-1} µg protein $^{-1}$. *$P < 0.05$ when compared with the values obtained in animals infected with the untreated yeast-like cells, or fungal cells preincubated with the preimmune serum.

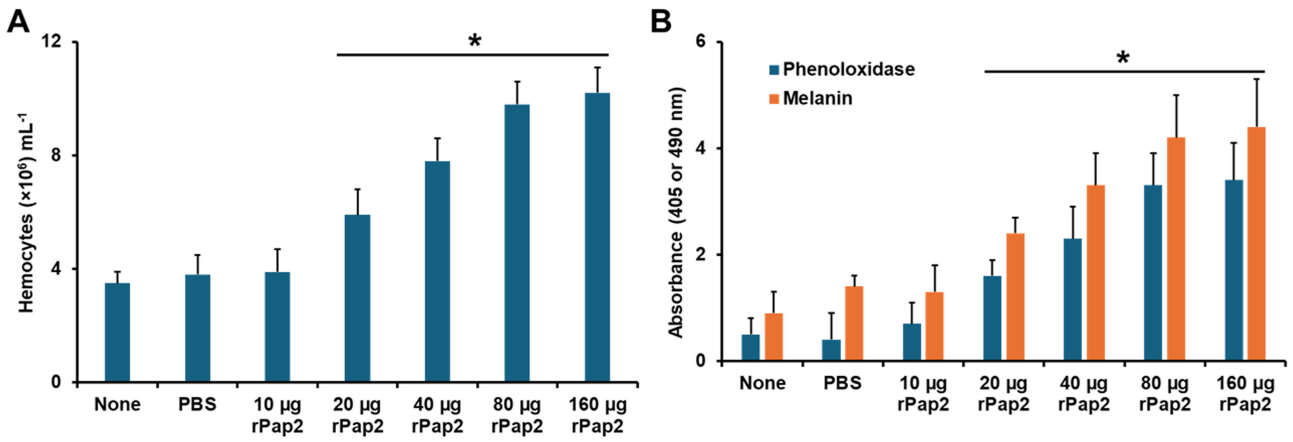

Figure 5 Immunological activation in *Galleria mellonella* by recombinant Pap2. Groups containing 30 larvae were injected with phosphate-buffered saline (PBS) or the indicated amount of rPap2, incubated for 5 days at 37°C, and decapitated for hemolymph collection. None, refers to a larva group that was not manipulated. In (**A**) hemolymph was used to quantify the levels of hemocytes. In (**B**) hemolymph was used to quantify melanin production and phenoloxidase activity. The former was defined as the absorbance at 405 nm of the cell-free hemolymph, whilst for the latter, enzyme activity was defined as the Δ_{490nm} min^{-1} µg $protein^{-1}$. The results are means ± SD of three independent experiments performed in duplicate. *$p < 0.05$ when compared to None or PBS groups.

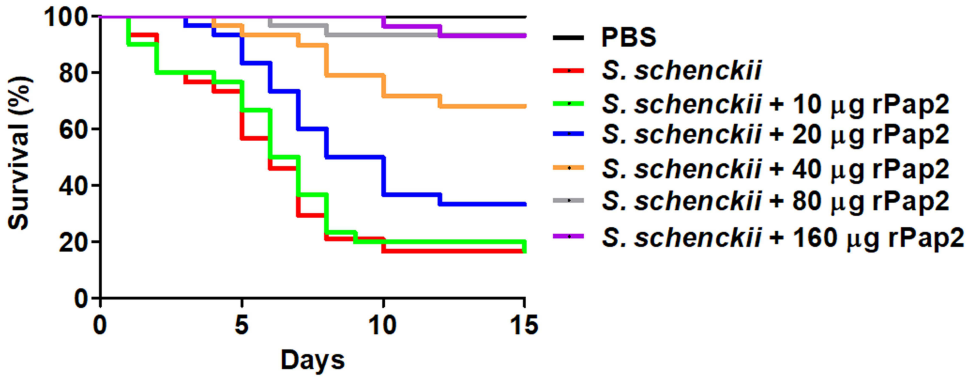

Figure 6 Effect of recombinant Pap2 on *Galleria mellonella* challenged with *Sporothrix schenckii* yeast-like cells. Groups of 30 *G. mellonella* larvae were inoculated with either phosphate-buffered saline (*S. schenckii*) or the indicated amount of rPap2 and incubated for 5 days at 37 °C. Then, a lethal inoculum of $1×10^5$ *S. schenckii* yeast-like cells was injected into larvae, kept at 37 °C, and mortality was recorded daily. PBS, control group inoculated and challenged with phosphate-buffered saline.

Discussion

The identification of virulence factors in members of the pathogenic clade of the *Sporothrix* genus is currently limited, and most of them are predictions based on other fungal species.[11,54] Adhesion is one of the early stages during colonization and invasion of host cells and tissues, and it is currently a common feature of fungal pathogens of medical relevance.[55,56] So, it is fundamental that *S. schenckii* has acquired proteins with adhesive properties during its evolutionary history. The results shown here are compatible with proposing Pap2 as a new *S. schenckii* adhesin, which is added

Table 3 Colony-Forming Units, Cytotoxicity, and Some Immunological Parameters in *Galleria mellonella* Larvae Pre-Inoculated with rPap2 and Challenged with *Sporothrix schenckii* Yeast-Like Cells

Inoculum[a]	Challenge[a]	Colony-Forming Units (x 10^5)[b]	Cytotoxicity (%)[c]	Hemocytes (×10^6) mL^{-1}	Melanin [d]	Phenoloxidase [e]
PBS [d]	PBS	0.0 ± 0.0	11.2 ± 3.5	3.7 ± 0.5	1.5 ± 0.5	0.2 ± 0.1
PBS	*S. schenckii*	4.7 ± 0.6	93.1 ± 6.5	8.8 ± 0.5	5.5 ± 0.6	4.2 ± 0.3
10 µg rPap2	*S. schenckii*	4.6 ± 0.5	90.9 ± 5.1	8.9 ± 0.6	5.3 ± 0.5	4.0 ± 0.3

(*Continued*)

https://doi.org/10.2147/IDR.S572598

Table 3 (Continued).

Inoculum[a]	Challenge[a]	Colony-Forming Units (x 10^5)[b]	Cytotoxicity (%)[c]	Hemocytes (×10^6) mL^{-1}	Melanin [d]	Phenoloxidase [e]
20 µg rPap2	*S. schenckii*	3.2 ± 0.5*	53.2 ± 7.7*	10.5 ± 0.4*	6.3 ± 0.3*	5.2 ± 0.5*
40 µg rPap2	*S. schenckii*	2.3 ± 0.4*	35.4 ± 7.1*	10.8 ± 0.2*	7.0 ± 0.4*	6.6 ± 0.7*
80 µg rPap2	*S. schenckii*	1.4 ± 0.5*	13.1 ± 4.5*	10.5 ± 0.5*	7.4 ± 0.4*	6.4 ± 0.3*
160 µg rPap2	*S. schenckii*	1.2 ± 0.5*	14.1 ± 8.8*	10.7 ± 0.4*	7.6 ± 0.2*	6.6 ± 0.8*

Notes: [a] The indicated inoculum was injected, larvae were incubated for 5 days at 37°C, and the indicated challenge was injected, and larvae were under observation for 15 days.[b] Hemolymph was withdrawn from decapitated larvae and used to quantify fungal colony-forming units by serial dilutions in YPD medium. [c] Lactate dehydrogenase activity was quantified in cell-free hemolymph. The 100% activity corresponds to data obtained with lysed hemocytes. [d] Quantified in the cell-free hemolymph as A_{405nm}. [e] Phenoloxidase activity defined as the Δ_{490nm} min^{-1} µg $protein^{-1}$. *$P < 0.05$ when compared with the values obtained in animals inoculated with PBS and challenged with *S. schenckii*.

to Gp70, Pap1, Hsp60, and Cbp1, currently the known cell wall adhesins in this organism.[20,21,25] Whether Pap2 acts in synergy with any of these adhesins, forming a heterogeneous complex or works as a sole component of the PRM in adhesion to host components, remains to be addressed.

As mentioned, Pap2 belongs to the PRM complex but does not have the typical traits of a secreted protein. The bioinformatics analysis indicates it lacks a signal peptide, a trait that most of the proteins that enter the endoplasmic reticulum contain as part of their primary structure.[57] However, the bioinformatic predictions indicate that Pap2 contains 3 and 13 putative *N*-linked and *O*-linked glycosylation sites, and this observation is in line with the experimental molecular weight of the native Pap2 and the fact that it belongs to PRM, a complex rich in glycoproteins.[20,30] Therefore, Pap2 should enter the endoplasmic reticulum lumen and transit the secretory pathway. The Pap2 translocation to the endoplasmic reticulum may be due to signal-peptide-independent mechanisms, such as those that recognize specific internal sequences within the protein.[58] Our bioinformatics strategy failed to propose an additional function to Pap2, suggesting this may be a protein with a sole function of adhesin. This contrasts with Gp70 and Hsp60, which are moonlighting proteins with a canonical biological function different from adhesion.[20,25] For these proteins, adhesive properties are observed when they are relocated within the cell wall. Thus, Pap1 and Pap2 are currently the non-moonlighting adhesins in *S. schenckii*.[20] Since we also detected Pap2 in the *S. brasiliensis* cell wall, we propose that in this organism Pap2 is performing similar functions as those described here for *S. schenckii*. However, this hypothesis remains to be confirmed.

One interesting observation is the adhesion profile to ECM components. Pap2 showed adhesion to laminin, elastin, fibrinogen, and fibronectin; while Hsp60 and Pap1 showed adhesion to these components and to type-I and type-II collagen.[20] Gp70 showed adhesion only to fibronectin and laminin.[25] This indicates that adhesion to some ECM components is redundant for these adhesins, suggesting the organism needs to establish adhesion to these components during the course of the infection. Laminin, elastin, and cellular fibronectin are abundant proteins in the cutaneous and subcutaneous tissues,[59–61] the primary points of contact of *S. schenckii* cells when interacting with the mammalian host.[8] One limitation of our study is that we currently cannot establish whether these proteins work independently or as part of a protein complex with adhesive properties.

The relevance of this protein for the interaction with the host was shown in the killing experiments in *G. mellonella* larvae. The protein backbone was capable of inducing immunological priming, suggesting this protein may be a candidate to explore its properties to generate long-lasting immunological memory that may protect against sporotrichosis. Currently, Gp70 is the only *S. schenckii* protein that has shown the ability to induce protection against experimental sporotrichosis.[62–65]

Although rPap2 immunization induced immune priming and conferred protection, conclusions regarding the generation of a long-term immunological memory in a susceptible mammalian host must be interpreted cautiously, because of the lack of an adaptive immune system in our model, *G. mellonella*. Our observations will require future validation in a murine model of experimental sporotrichosis. On the other hand, the exact proportion of Pap2 exposed on the fungal cell surface during different life cycle stages and its impact on in vivo adhesion are open questions that remain to be addressed.

Conclusion

In conclusion, we presented evidence indicating *S. schenckii* Pap2, a protein belonging to the cell wall PRM, has adhesive properties to ECM components and epithelial cells, and is required for the *S. schenckii* virulence in *G. mellonella* larvae.

Acknowledgments

We thank Luz A. López-Ramírez, MSc, for the technical assistance in this project.

Funding

This work was supported by Secretaría de Ciencia, Humanidades, Tecnología e Innovación [Ciencia de Frontera 2019-6380 and CBF2023-2024-655], Universidad de Guanajuato [CIIC-2025-201/2025], and Red Temática Glicociencia en Salud [CONACYT-México]. The funders had no role in the design of the study; in the collection, analyses, or interpretation of data; in the writing of the manuscript, or in the decision to publish the results.

Disclosure

The authors declare no conflicts of interest in this work.

References

1. Lopez-Romero E, Reyes-Montes MDR, Perez-Torres A, et al. *Sporothrix schenckii* Complex And Sporotrichosis, An Emerging Health Problem. *Future Microbiol*. 2011;6(1):85–102. doi:10.2217/fmb.10.157
2. Nava-Pérez N, Neri-García LG, Romero-González OE, Terrones-Cruz JA, García-Carnero LC, Mora-Montes HM. Biological and clinical attributes of *Sporothrix globosa*, a causative agent of sporotrichosis. *Infect Drug Resist*. 2022;15:2067–2090. doi:10.2147/idr.s362099
3. Gómez-Gaviria M, Martínez-Álvarez JA, Mora-Montes HM. Current progress in *Sporothrix brasiliensis* basic aspects. *J Fungi*. 2023;9(5):533.
4. Chakrabarti A, Bonifaz A, Gutierrez-Galhardo MC, Mochizuki T, Li S. Global epidemiology of sporotrichosis. *Med Mycol*. 2015;53(1):3–14. doi:10.1093/mmy/myu062
5. Fuchs T, Visagie CM, Wingfield BD, Wingfield MJ. *Sporothrix* and Sporotrichosis: a South African perspective on a growing global health threat. *Mycoses*. 2024;67(10):e13806. doi:10.1111/myc.13806
6. Sendrasoa FA, Ratovonjanahary VT, Ranaivo IM, et al. Epidemiological and clinical aspects of sporotrichosis in patients seen at a reference hospital in Madagascar. *PLoS Negl Trop Dis*. 2023;17(7):e0011478. doi:10.1371/journal.pntd.0011478
7. Santos MT, Nascimento LFJ, Barbosa AAT, et al. The rising incidence of feline and cat-transmitted sporotrichosis in Latin America. *Zoonoses Public Health*. 2024;71(6):609–619. doi:10.1111/zph.13169
8. Barros MB, de Almeida Paes R, Schubach AO. *Sporothrix schenckii* and sporotrichosis. *Clin Microbiol Rev*. 2011;24(4):633–654. doi:10.1128/cmr.00007-11
9. Marimon R, Cano J, Gené J, Sutton DA, Kawasaki M, Guarro J. *Sporothrix brasiliensis, S. globosa*, and *S. mexicana*, three new *Sporothrix* species of clinical interest. *J Clin Microbiol*. 2007;45:3198–3206. doi:10.1128/jcm.00808-07
10. Mora-Montes HM, Dantas Ada S, Trujillo-Esquivel E, de Souza Baptista AR, Lopes-Bezerra LM, Munro C. Current progress in the biology of members of the *Sporothrix schenckii* complex following the genomic era. *FEMS Yeast Res*. 2015;15(6):fov065. doi:10.1093/femsyr/fov065
11. Tamez-Castrellón AK, Romeo O, García-Carnero LC, Lozoya-Pérez NE, Mora-Montes HM. Virulence factors in *Sporothrix schenckii*, one of the causative agents of sporotrichosis. *Curr Protein Pept Sci*. 2020;21(3):295–312. doi:10.2174/1389203720666191007103004
12. Ikeda MAK, de Almeida JRF, Jannuzzi GP, et al. Extracellular vesicles from *Sporothrix brasiliensis* are an important virulence factor that induce an increase in fungal burden in experimental sporotrichosis. *Front Microbiol*. 2018;9:2286. doi:10.3389/fmicb.2018.02286
13. Sandoval-Bernal G, Barbosa-Sabanero G, Shibayama M, Perez-Torres A, Tsutsumi V, Sabanero M. Cell wall glycoproteins participate in the adhesion of Sporothrix schenckii to epithelial cells. *Mycopathologia*. 2011;171(4):251–259. doi:10.1007/s11046-010-9372-8
14. Figueiredo CC, De Lima OC, De Carvalho L, Lopes-Bezerra LM, Morandi V. The *in vitro* interaction of *Sporothrix schenckii* with human endothelial cells is modulated by cytokines and involves endothelial surface molecules. *Microb Pathog*. 2004;36(4):177–188. doi:10.1016/j.micpath.2003.11.003
15. Sánchez-Herrera R, Flores-Villavicencio LL, Pichardo-Molina JL, et al. Analysis of biofilm formation by *Sporothrix schenckii*. *Med Mycol*. 2021;59(1):31–40. doi:10.1093/mmy/myaa027
16. Brilhante RSN, Fernandes MR, Pereira VS, et al. Biofilm formation on cat claws by *Sporothrix* species: an *ex vivo* model. *Microb Pathog*. 2021;150:104670. doi:10.1016/j.micpath.2020.104670
17. Lima OC, Figueiredo CC, Pereira BA, Coelho MG, Morandi V, Lopes-Bezerra LM. Adhesion of the human pathogen *Sporothrix schenckii* to several extracellular matrix proteins. *Braz J Med Biol Res*. 1999;32(5):651–657. doi:10.1590/s0100-879x1999000500020
18. Lima OC, Bouchara JP, Renier G, Marot-Leblond A, Chabasse D, Lopes-Bezerra LM. Immunofluorescence and flow cytometry analysis of fibronectin and laminin binding to *Sporothrix schenckii* yeast cells and conidia. *Microb Pathog*. 2004;37(3):131–140. doi:10.1016/j.micpath.2004.06.005
19. Lima OC, Figueiredo CC, Previato JO, Mendonça-Previato L, Morandi V, Lopes Bezerra LM. Involvement of fungal cell wall components in adhesion of Sporothrix schenckii to human fibronectin. *Infect Immun*. 2001;69(11):6874–6880. doi:10.1128/iai.69.11.6874-6880.2001
20. García-Carnero LC, Salinas-Marín R, Lozoya-Pérez NE, et al. The Heat shock protein 60 and Pap1 participate in the *Sporothrix schenckii*-host interaction. *J Fungi*. 2021;7(11):960. doi:10.3390/jof7110960

21. Contreras-López LM, Ramírez-Sotelo U, Martínez-Duncker I, Franco B, Mora-Montes HM. The Cbp1 protein is a peptidorhamnomannan adhesin that contributes to the *Sporothrix schenckii* virulence. *Fungal Biology*. 2025;129(8):101682. doi:10.1016/j.funbio.2025.101682
22. Procópio-Azevedo AC, de Abreu Almeida M, Almeida-Paes R, et al. The state of the art in transcriptomics and proteomics of clinically relevant *Sporothrix* species. *J Fungi*. 2023;9(8):790. doi:10.3390/jof9080790
23. Ruiz-Baca E, Toriello C, Pérez-Torres A, Sabanero-López M, Villagómez-Castro JC, López-Romero E. Isolation and some properties of a glycoprotein of 70 kDa (Gp70) from the cell wall of *Sporothrix schenckii* involved in fungal adherence to dermal extracellular matrix. *Med Mycol*. 2009;47(2):185–196. doi:10.1080/13693780802165789
24. Teixeira PAC, de Castro RA, Nascimento RC, et al. Cell surface expression of adhesins for fibronectin correlates with virulence in *Sporothrix schenckii*. *Microbiology*. 2009;155(11):3730–3738. doi:10.1099/mic.0.029439-0
25. López-Ramírez LA, Martínez-Álvarez JA, Martínez-Duncker I, Lozoya-Pérez NE, Mora-Montes HM. Silencing of *Sporothrix schenckii GP70* reveals its contribution to fungal adhesion, virulence, and the host-fungus interaction. *J Fungi*. 2024;10(5):302. doi:10.3390/jof10050302
26. Padró-Villegas L, Gómez-Gaviria M, Martínez-Duncker I, et al. *Sporothrix brasiliensis* Gp70 is a cell wall protein required for adhesion, proper interaction with innate immune cells, and virulence. *Cell Surface*. 2025;13:100139. doi:10.1016/j.tcsw.2024.100139
27. Gómez-Gaviria M, Martínez-Álvarez JA, Martínez-Duncker I, Baptista ARS, Mora-Montes HM. Silencing of *MNT1* and *PMT2* shows the importance of *O*-linked glycosylation during the *Sporothrix schenckii*-host interaction. *J Fungi*. 2025;11(5):352. doi:10.3390/jof11050352
28. Lopes-Bezerra LM, Walker LA, Niño-Vega G, et al. Cell walls of the dimorphic fungal pathogens *Sporothrix schenckii* and *Sporothrix brasiliensis* exhibit bilaminate structures and sloughing of extensive and intact layers. *PLoS Negl Trop Dis*. 2018;12(3):e0006169–e0006169. doi:10.1371/journal.pntd.0006169
29. Villalobos-Duno HL, Barreto LA, Alvarez-Aular Á, et al. Comparison of cell wall polysaccharide composition and structure between strains of *Sporothrix schenckii* and *Sporothrix brasiliensis*. *Front Microbiol*. 2021;12:726958. doi:10.3389/fmicb.2021.726958
30. Lopes-Bezerra LM. *Sporothrix schenckii* cell wall peptidorhamnomannans. Mini Review. *Front Microbiol*. 2011;2:243. doi:10.3389/fmicb.2011.00243
31. Castro RA, Kubitschek-Barreira PH, Teixeira PAC, et al. Differences in cell morphometry, cell wall topography and Gp70 expression correlate with the virulence of *Sporothrix brasiliensis* clinical isolates. *PLoS One*. 2013;8(10):e75656.
32. Madrid H, Cano J, Gené J, Bonifaz A, Toriello C, Guarro J. *Sporothrix globosa*, a pathogenic fungus with widespread geographical distribution. *Rev Iberoam Micol*. 2009;26(3):218–222. doi:10.1016/j.riam.2009.02.005
33. Martínez-Álvarez JA, Pérez-García LA, Mellado-Mojica E, et al. *Sporothrix schenckii sensu stricto* and *Sporothrix brasiliensis* are differentially recognized by human peripheral blood mononuclear cells. *Front Microbiol*. 2017;8:843. doi:10.3389/fmicb.2017.00843
34. Trujillo-Esquivel E, Franco B, Flores-Martínez A, Ponce-Noyola P, Mora-Montes HM. Purification of single-stranded cDNA based on RNA degradation treatment and adsorption chromatography. *Nucleosides Nucleotides Nucleic Acids*. 2016;35(8):404–409. doi:10.1080/15257770.2016.1184277
35. Ramírez-Sotelo U, García-Carnero LC, Martínez-Álvarez JA, Gómez-Gaviria M, Mora-Montes HM. An ELISA-based method for *Galleria mellonella* apolipophorin-III quantification. *PeerJ*. 2024;12:e17117. doi:10.7717/peerj.17117
36. Hager DA, Burgess RR. Elution of proteins from sodium dodecyl sulfate-polyacrylamide gels, removal of sodium dodecyl sulfate, and renaturation of enzymatic activity: results with sigma subunit of Escherichia coli RNA polymerase, wheat germ DNA topoisomerase, and other enzymes. *Anal Biochem*. 1980;109(1):76–86. doi:10.1016/0003-2697(80)90013-5
37. Chevallet M, Luche S, Rabilloud T. Silver staining of proteins in polyacrylamide gels. *Nat Protoc*. 2006;1(4):1852–1858. doi:10.1038/nprot.2006.288
38. Mora-Montes HM, Bader O, López-Romero E, et al. Kex2 protease converts the endoplasmic reticulum alpha1,2-mannosidase of *Candida albicans* into a soluble cytosolic form. *Microbiology*. 2008;154(Pt 12):3782–3794. doi:10.1099/mic.0.2008/019315-0
39. Consortium TU. UniProt: the Universal Protein Knowledgebase in 2023. *Nucleic Acids Res*. 2022;51(D1):D523–D531. doi:10.1093/nar/gkac1052
40. Liu Y, Yang X, Gan J, Chen S, Xiao ZX, Cao Y. CB-Dock2: improved protein-ligand blind docking by integrating cavity detection, docking and homologous template fitting. *Nucleic Acids Res*. 2022;50(W1):W159–w164. doi:10.1093/nar/gkac394
41. Yan Y, Tao H, He J, Huang S-Y. The HDOCK server for integrated protein–protein docking. *Nature Protocols*. 2020;15(5):1829–1852. doi:10.1038/s41596-020-0312-x
42. Clavijo-Giraldo DM, Matinez-Alvarez JA, Lopes-Bezerra LM, et al. Analysis of *Sporothrix schenckii sensu stricto* and *Sporothrix brasiliensis* virulence in *Galleria mellonella*. *J Microbiol Methods*. 2016;122:73–77. doi:10.1016/j.mimet.2016.01.014
43. García-Carnero LC, Clavijo-Giraldo DM, Gómez-Gaviria M, et al. Early virulence predictors during the *Candida* species-*Galleria mellonella* Interaction. *J Fungi*. 2020;6(3):152. doi:10.3390/jof6030152
44. Lozoya-Pérez NE, Clavijo-Giraldo DM, Martínez-Duncker I, et al. Influences of the culturing media in the virulence and cell wall of *Sporothrix schenckii*. *J Fungi*. 2020;6(4):323. doi:10.3390/jof6040323
45. Mészáros B, Erdos G, Dosztányi Z. IUPred2A: context-dependent prediction of protein disorder as a function of redox state and protein binding. *Nucleic Acids Res*. 2018;46(W1):W329–w337. doi:10.1093/nar/gky384
46. Omasits U, Ahrens CH, Müller S, Wollscheid B. Protter: interactive protein feature visualization and integration with experimental proteomic data. *Bioinformatics*. 2014;30(6):884–886. doi:10.1093/bioinformatics/btt607
47. Gasteiger E, Hoogland C, Gattiker A, et al. Protein identification and analysis tools on the ExPASy server. In: Walker JM, editor. *The Proteomics Protocols Handbook*. Humana Press; 2005. 571–607.
48. Chen C, Zabad S, Liu H, Wang W, Jeffery C. MoonProt 2.0: an expansion and update of the moonlighting proteins database. *Nucleic Acids Res*. 2018;46(D1):D640–d644. doi:10.1093/nar/gkx1043
49. Finn RD, Clements J, Arndt W, et al. HMMER web server: 2015 update. *Nucleic Acids Res*. 2015;43(W1):W30–38. doi:10.1093/nar/gkv397
50. Madeira F, Madhusoodanan N, Lee J, et al. The EMBL-EBI Job Dispatcher sequence analysis tools framework in 2024. *Nucleic Acids Res*. 2024;52(W1):W521–W525. doi:10.1093/nar/gkae241
51. Martínez-Álvarez JA, García-Carnero LC, Kubitschek-Barreira PH, et al. Analysis of some immunogenic properties of the recombinant *Sporothrix schenckii* Gp70 expressed in *Escherichia coli*. *Future Microbiol*. 2019;14:397–410. doi:10.2217/fmb-2018-0295
52. Wu G, Yi Y, Lv Y, Li M, Wang J, Qiu L. The lipopolysaccharide (LPS) of *Photorhabdus luminescens* TT01 can elicit dose- and time-dependent immune priming in *Galleria mellonella* larvae. *J Invertebr Pathol*. 2015;127:63–72. doi:10.1016/j.jip.2015.03.007

53. Bidla G, Hauling T, Dushay MS, Theopold U. Activation of insect phenoloxidase after injury: endogenous versus foreign elicitors. *J Innate Immun*. 2009;1(4):301–308. doi:10.1159/000168009
54. García-Carnero LC, Martínez-Álvarez JA. Virulence factors of *Sporothrix schenckii*. *J Fungi*. 2022;8(3):318. doi:10.3390/jof8030318
55. Kumari A, Tripathi AH, Gautam P, et al. Adhesins in the virulence of opportunistic fungal pathogens of human. *Mycology*. 2021;12(4):296–324. doi:10.1080/21501203.2021.1934176
56. Timmermans B, De Las Peñas A, Castaño I, Van Dijck P. Adhesins in *Candida glabrata*. *J Fungi*. 2018;4(2):60. doi:10.3390/jof4020060
57. Owji H, Nezafat N, Negahdaripour M, Hajiebrahimi A, Ghasemi Y. A comprehensive review of signal peptides: structure, roles, and applications. *Eur J Cell Biol*. 2018;97(6):422–441. doi:10.1016/j.ejcb.2018.06.003
58. Rabouille C. Pathways of unconventional protein secretion. *Trends Cell Biol*. 2017;27(3):230–240. doi:10.1016/j.tcb.2016.11.007
59. To WS, Midwood KS. Plasma and cellular fibronectin: distinct and independent functions during tissue repair. *FibrogenTissue Repair*. 2011;4(1):21. doi:10.1186/1755-1536-4-21
60. Sage EH, Gray WR. Evolution of elastin structure. In: Sandberg LB, Gray WR, Franzblau C, editors. *Elastin and Elastic Tissue*. Springer US; 1977:291–312.
61. Aumailley M. The laminin family. *Cell Adh Migr*. 2013;7(1):48–55. doi:10.4161/cam.22826
62. de Almeida JR, Kaihami GH, Jannuzzi GP, de Almeida SR. Therapeutic vaccine using a monoclonal antibody against a 70-kDa glycoprotein in mice infected with highly virulent *Sporothrix schenckii* and *Sporothrix brasiliensis*. *Med Mycol*. 2015;53(1):42–50. doi:10.1093/mmy/myu049
63. de Almeida JR, Santiago KL, Kaihami GH, Maranhão AQ, de Macedo Brígido M, de Almeida SR. The efficacy of humanized antibody against the *Sporothrix* antigen, gp70, in promoting phagocytosis and reducing disease burden. *Front Microbiol*. 2017;8:345. doi:10.3389/fmicb.2017.00345
64. de Almeida JRF, Jannuzzi GP, Kaihami GH, Breda LCD, Ferreira KS, de Almeida SR. An immunoproteomic approach revealing peptides from *Sporothrix brasiliensis* that induce a cellular immune response in subcutaneous sporotrichosis. *Sci Rep*. 2018;8(1):4192. doi:10.1038/s41598-018-22709-8
65. de Almeida SR. Advances in vaccine development against sporotrichosis. *Curr Trop Med Rep*. 2019;6(3):126–131. doi:10.1007/s40475-019-00183-0